Mass Spectrometry
DOI: 10.5702/massspectrometry.A0164
Vol. 13 (2024), A0164

Original Article

Imaging Lipidomics and Metallomics of Brown Rice Cultivars Used for Sake Production

Eliza Farestiani[1], Yoshihiro Tamada[1,2], Koji Okuda[3], Eiichiro Fukusaki[1,4,5], and Shuichi Shimma[*,1,4,5]

[1]*Department of Biotechnology, Graduate School of Engineering, Osaka University, 2–1 Yamadaoka, Suita, Osaka 565–0871, Japan*
[2]*Hakutsuru Sake Brewing Co., Ltd., 4–5–5 Sumiyoshiminami-machi, Higashinada-ku, Kobe 658–0041, Japan*
[3]*Solutions COE, Analytical and Measuring Instruments Division, Shimadzu Corporation, Nishinokyo Kuwabaracho 1, Nakagyo-ku, Kyoto 604–8442, Japan*
[4]*Institute for Open and Transdisciplinary Research Initiatives, Osaka University, 2–1 Yamadaoka, Suita, Osaka 565–0871, Japan*
[5]*Osaka University Shimadzu Omics Innovation Research Laboratory, Osaka University, 2–1 Yamadaoka, Suita, Osaka 565–0871, Japan*

Many previous studies have reported various phospholipids and elements that affect sake production; however, it seems to be challenging to investigate individual types in each rice variety due to their high diversity, not to mention their distribution patterns. Since its introduction, mass spectrometry imaging (MSI) has gained attention in various fields as a simple compound visualization technique. The current study highlights the progress of powerful MSI in comprehensively analyzing phospholipids and minerals in brown rice for sake production. Multivariate analysis suggested phospholipids relating to each rice group based on regions of interest. Phospholipid classes connected with embryo and endosperm included fatty acylcarnitine, diacylglycerol, phosphatidylcholine, phosphatidylglycerol, and phosphatidylethanolamine. Meanwhile, the studied rice groups showed the same distribution of the investigated 12 minerals. This is the first study that reports a comprehensive imaging analysis of phospholipids and elements in brown rice for several cultivars for sake production.

Please cite this article as: Mass Spectrom (Tokyo) 2024; 13(1): A0164

Keywords: sake rice, general rice, lipids, metals, mass spectrometry imaging

(Received August 28, 2024; Accepted November 28, 2024; advance publication released online December 10, 2024)

INTRODUCTION

Sake is a national alcoholic beverage of Japan which is brewed from rice (*Oryza sativa* L.) as the main constituent through a unique process, simultaneously parallel bioconversions, during which the starch of rice is decomposed by *koji* starter (*Aspergillus oryzae*) liberating sugars to be then fermented into alcohol by yeast *Saccharomyces cerevisiae*.[1)] As the principal material, the suitability of rice for sake production is an important consideration. The rice used in the sake industry is characteristically different from general rice. Sake rice cultivars have some special features, including larger grain size and weight that reasonably represent a higher rate of white-core region (so-called *shinpaku*) expression (WCE) in the center part of rice grain.[2)] Larger *shinpaku* indirectly contributes to brewing high-quality sake because this property is thought to be important for the growth of *koji* mold and enhances the digestibility and gelatinization of the rice.[3–5)] In addition, brewing rice cultivars are also characterized by lower content of protein, lipid, and several inorganic compounds that, when in an excess amount, contribute to sake deterioration such as a rough taste, coloration, and unpleasant aroma.[1)]

In particular, about 2%–3% of lipid is contained in rice grain with dominant accumulation in the rice bran (19.4%–25.5%) and germ (34.1%–36.5%), while only 0.8% in the endosperm.[6,7)] As mentioned above, in the sake industry, it is well known that lipids are one of the main concerns. Among all rice lipids categories, phospholipids are a major lipid constituent that accounts for approximately 10% of the total rice lipid content[7)] from which unsaturated fatty acids are derived and increased, which negatively impacts the pathway of fermentation in *S. cerevisiae*.[8)] The presence of unsaturated fatty acids leads to the inhibition of the biosynthesis of isoamyl acetate (banana-like aroma) and ethyl caproate (apple-like aroma) in *S. cerevisiae*[9)] which are important

*Correspondence to: Shuichi Shimma, *Department of Biotechnology, Graduate School of Engineering, Osaka University, 2–1 Yamadaoka, Suita, Osaka 565–0871, Japan*, e-mail: sshimma@bio.eng.osaka-u.ac.jp

aroma-enhancing components in sake are reduced, directly deteriorating sake's flavor quality. The inhibitory effect was also consistent with a study by Furukawa *et al.*[10] when phospholipids phosphatidylinositol (PI), phosphatidylcholine (PC), phosphatidylglycerol (PG), and phosphatidylethanolamine (PE) were examined in sake mash. Aside from the effect on the involved enzyme, fatty acids derived from phospholipids could also alter volatile compositions and generate some undesirable compounds. A previous study showed medium-chain fatty acids (MCFAs) such as hexanoic acid, octanoic acid, and butanoic acid, MCFA derivatives, and long-chain alkanes produced from MCFA decarboxylation reaction contributed to fatty odor and inharmonious taste in sake.[11,12] For these reasons, phospholipids are undesired for sake manufacturing.

It is also important not to disregard inorganic elements, despite comprising merely approximately 1% of brown rice.[1] Several minerals such as potassium (K), magnesium (Mg), and phosphorus (P) are essential for supporting the quality of *koji*, the fermentation process, and the growth of brewing microorganisms, while sulfur (S), iron (Fe), and manganese (Mn) are thought to be greatly responsible as a causative agent of coloration in sake.[13] Both raw rice and water contain such inorganic elements, but regardless of the sources, it is unnecessary to allow low levels of all elements during the sake-making process. Several works have reported how some inorganic components interfered with sake's quality.[14,15] Among the studies that have been carried out so far, the investigations have worked on the effects derived from minerals on unpleasant taste, coloration, and the increasing of off-flavor compounds in the sake product.[16–18] Unfortunately, specific analysis on minerals in rice grains for sake manufacturing remains limited to the total concentration (in ppm),[13,19] the effect of polishing,[20] and the impact on rice digestibility.[21]

While it is possible to eliminate the unwanted components by the rice polishing process, some concerns remain unresolved. Even though phospholipids and minerals-related works in sake brewing have been performed for years, there remains a lack of information on the diversity of phospholipids and minerals present in rice grains exclusively processed for sake production, leading to uncertainty about the occurrence of specific phospholipids and minerals to certain rice cultivars. Following this, it is sufficiently clear that up to the present, the exact distribution of phospholipids and minerals in rice tissues subjected to sake-making also remains unclear. Consequently, it is difficult to ascertain whether these components can be perfectly removed or remain present even after the polishing treatment. Such concerns also apply to the fact that sake manufacturers utilize both sake rice and general rice. Nevertheless, it is still uncertain whether these different rice groups possess distinct or similar phospholipids and mineral profiles. Therefore, the information of their distribution may be worth acquiring.

Mass spectrometry imaging (MSI) is one of the analytical tools for metabolomic study that enables a wide range of metabolites in biological samples to be visible. Since its emergence, MSI has been applied well in various study fields, including medical and pharmaceutical,[22–25] enzyme histochemistry,[26–28] plant,[29,30] and even in the microbiological study,[31,32] to name a few. Furthermore, MSI has also been rapidly gaining popularity in food science[33–35] due to its power to localize numerous metabolites with different functions that benefit improving food quality, safety, and security. Other than that, methods for data analysis have also been optimized for deeper data elucidation, considering that the acquired information of the MSI data set is immensely high. For example, principal component analysis (PCA) has been employed to discriminate metabolite accumulation based on regions. This approach showed successful implementation in the previous reports.[36,37] Notwithstanding the significant advancements in this technique, only a few studies implemented sake brewing science, especially for raw material which is a significant starting point. Currently, the investigations are still restricted to the examination of rice *koji* [28,38,39] and one specific rice phospholipid.[40] Unfortunately, a comprehensive analysis of critical substances in rice for the production of sake has not yet been performed.

In light of this, in this current study, the application of MSI has been updated by comprehensively investigating and visualizing the distribution of phospholipids and minerals in rice cultivars used for sake production through widely targeted analysis. Utilizing region of interest (ROI)-based PCA in rice cultivars for sake production, mass spectra that were detected to be highly correlated with a particular region were subjected to further analysis on an individual basis. The findings of this study are expected to be not only useful in advancing scientific knowledge of brewing but also in potentially benefiting the sake industry, specifically in the selection of rice cultivars and the polishing process.

EXPERIMENTAL

Samples information

Brown rice (polishing ratio of 100%) of sake rice (*Hakutsurunishiki* and *Yamadanishiki*) and general rice (*Yamadawara*, *Nakate Shinsenbon*, and *Nipponbare*) were obtained from Hakutsuru Sake Brewing Co. Ltd. (Hyogo, Japan). *Hakutsurunishiki* and *Yamadanishiki* rice were cultivated in Hyogo, Japan in 2021, while *Yamadawara*, *Nakate Shinsenbon*, and *Nipponbare* were produced in Yamaguchi, Japan in 2022 (Table S1).

Preparation of rice sections

The experimental workflow of matrix-assisted laser desorption/ionization (MALDI) MSI in this current study is briefly summarized in Fig. 1. Rice sections were prepared by embedding the whole rice grains in molds (Base mold A, Falma, Tokyo, Japan) filled with 4% carboxymethyl cellulose (CMC) solution (Leica Microsystems, Wetzlar, Germany), followed by flash-freezing at −80°C. The frozen samples were transferred to a cryostat (CM1950, Leica Biosystems, Wetzlar, Germany) and sectioned into 16 μm at −22°C. The rice sections were collected using a cyrofilm (Section-Lab, Yokohama, Japan) and dried using silica gel (Fujifilm Wako Pure Chemical Corporation, Osaka, Japan) in a falcon tube (Corning, NY, USA) before being attached to an indium-tin-oxide (ITO)-coated glass slide (Matsunami, Osaka, Japan) using conductive double-sided tape (3M, Tokyo, Japan) for phospholipid imaging. As for mineral distribution, the rice sample sections with the same thickness were fixed on the general glass slide (Matsunami, Osaka, Japan) using general tape (Nichiban, Tokyo, Japan).

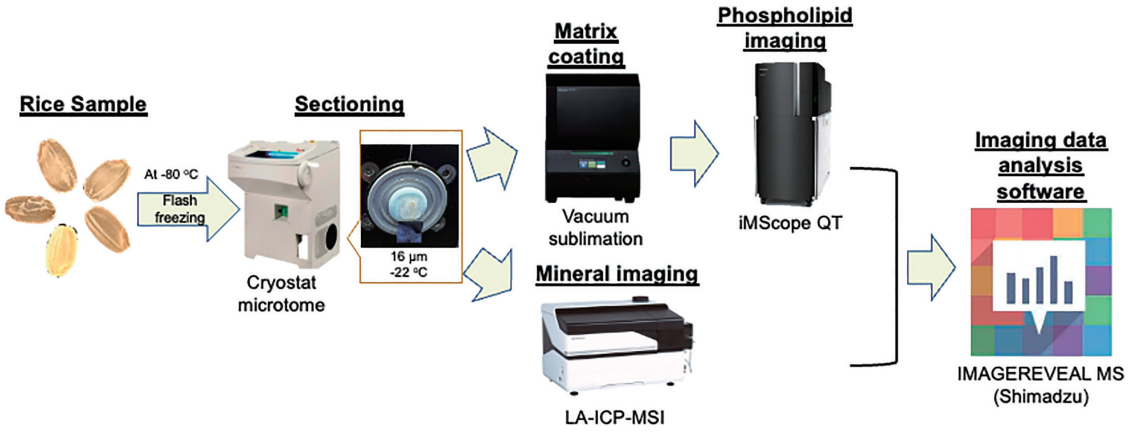

Fig. 1. Overview of MALDI MSI experimental workflow. MALDI, matrix-assisted laser desorption/ionization; MSI, mass spectrometry imaging.

Matrix deposition

To find a suitable matrix, 2 types of common matrices were used: α-cyano-4-hydroxycinnamic acid (CHCA) and 2,5-dihydroxybenzoic acid (DHB) (Merck, Darmstat, Germany). The matrices were separately deposited on ITO glass loaded with rice sections by sublimation method using matrix vapor deposition device iMLayer™ (Shimadzu, Kyoto, Japan) with the following conditions: CHCA with a thickness of 0.7 µm at 180°C; DHB with a thickness of 1.5 µm at 250°C.

MSI analysis

For phospholipid distribution, the analysis was performed using an iMScope™ QT (Shimadzu, Kyoto, Japan) with MALDI as an ion source. Mass spectra were recorded by Imaging MS Solution version 2.0 software, and all spectra were acquired in the *m/z* range of 500–1000 in the positive ionization mode. Laser diameter was set to 2. Other related conditions were as follows: Number of irradiations, 50 shots; Laser repetition rate, 1000 Hz; Laser strength, 67; Detector voltage, 2.30 kV; A pitch of 25 × 25 µm^2. After spectra data acquisition, the IMAGEREVEAL MS™ Software (Shimadzu, Kyoto, Japan) was utilized to generate phospholipid imaging data.

For mineral distribution, the rice sample sections were processed using laser ablation-inductivity coupled plasma (LA-ICP)-MSI technology (ICPMS-2030 and Laser ablation NWR266, Shimadzu, Kyoto, Japan). The parameters of ICPMS were set to high-frequency power, 1.20 kW; sampling depth, 5.0 mm; plasma gas flow rate, 9.0 L/min; auxiliary gas flow rate, 0.70 L/min; carrier gas flow rate, 0.40 L/min; chamber temperature, 5°C; peristaltic pump speed, 20 rpm; collision gas, He; cell gas flow rate, 6.0 mL/min; cell voltage, −21 V; and energy filter, 7.0 V. Meanwhile, laser ablation parameters were laser energy, 25%; laser irradiation diameter, 30 µm; scanning speed, 30 µm/sec; laser frequency, 1000 Hz; and He flow rate, 0.80 L/min.

Data analysis

After the mass spectra were generated, the data were then processed using IMAGEREVEAL MS™ for collective image analysis. At first, it was desirable to search for regions that share general similarities in their mass spectra before determining ROIs. The following were parameters set in the pre-processing settings: normalization; total ion current (TIC), target; lipids with *m/z* range 500–1000, number of clusters; 10, linkage criteria; ward, metric; Euclidean distance, data point thinning; none, delta *m/z*; ±0.01 Da. Based on the segmentation formed in each cluster of pixels, embryo and endosperm were selected as ROIs, as illustrated in Fig. S1, to be then subjected to the differential analysis. The number of analysis points per ROI was set to 3. From the test, the score plot and loading plot of PCA will be constructed to assist MALDI MSI data interpretation. Then, ion images were generated based on data points presented in the loading plots using the in-house database previously reported.

RESULTS AND DISCUSSION

Segmentation analysis of phospholipids localized in sake rice and general rice

During the MSI data analysis, many areas of the sample tissues corresponding to specific anatomical parts could be virtually specified.[41] A precise characterization approach of ROIs enables the delineation of tissue region-type specific compound accumulation, which is crucial for downstream statistical analysis.[42] For this reason, prior to the determination of ROI, segmentation analysis was carried out in all rice grain sections as a promising data-driven technique to define the pattern of localized features of the vast amount of analyte mass in tissue imaging data. In this examination, a clustering algorithm will separate a series of mass spectral profiles collected at different points of sample tissue sections into several groups, resulting in signal-based images from the whole mass range, thus weighted to reflect the variations across the ROIs. The analysis result visually showed not only specific location but also both distinct and similar accumulations of phospholipids between sake rice and general rice cultivars. According to the visual segmentation (Fig. 2), 2 ROIs of 10 clusters formed were further objectively analyzed by multivariate analysis.

Region-based differential analysis on the phospholipids distribution in sake rice and general rice

The data matrix obtained from each ROI (embryo and endosperm) was utilized for PCA plot construction. The PCA

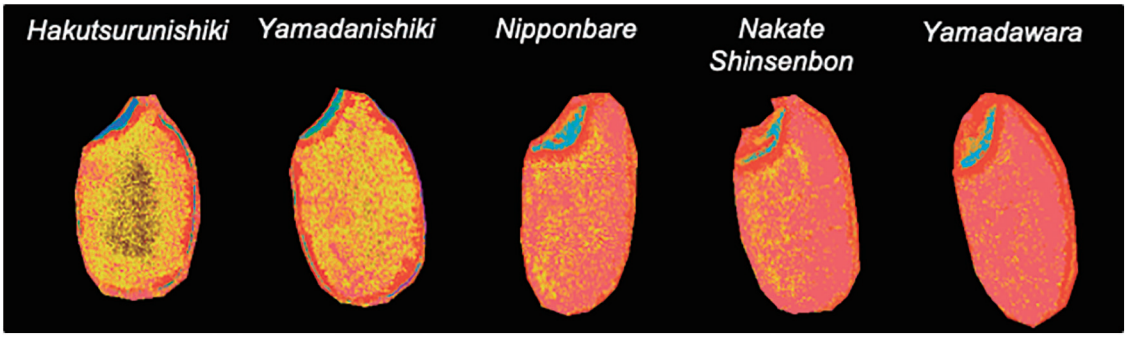

Fig. 2. Segmentation analysis showing the internal structure of sake rice and general rice based on phospholipid distribution. Different colors highlight the unique characteristics of the localization pattern.

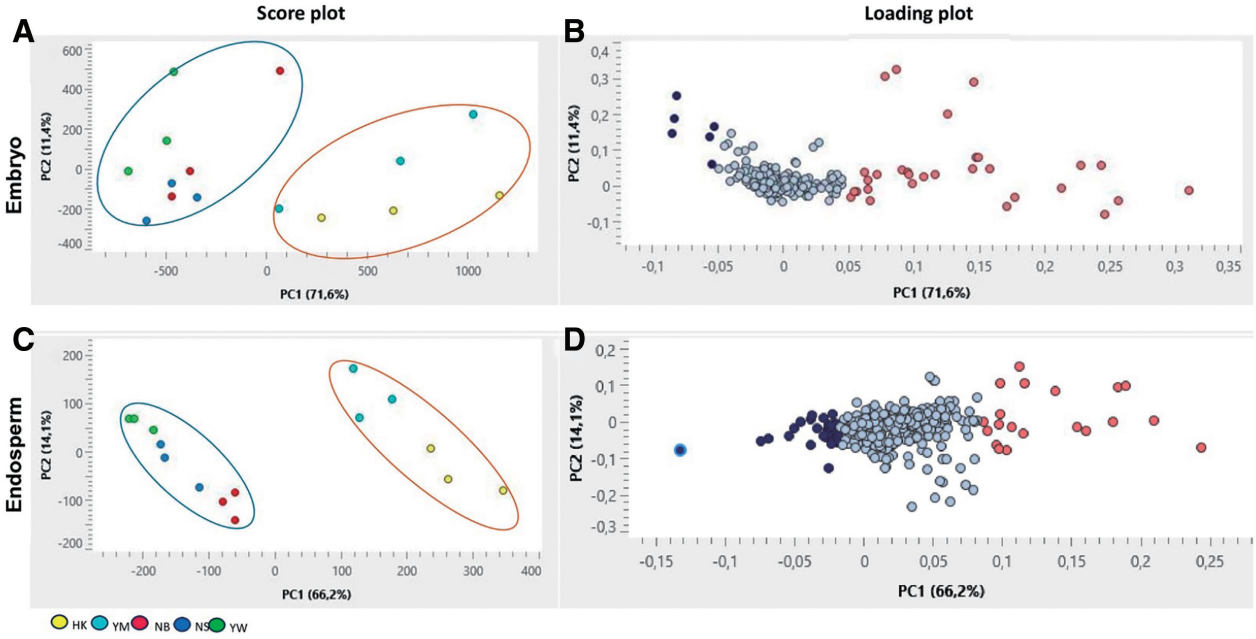

Fig. 3. PCA results of phospholipids in sake rice and general rice. (A) Score plot of phospholipids distribution in embryo part. (B) Loading plot representing phospholipids associated with each rice group embryo. (C) Score plot of phospholipids distribution in endosperm part. (D) Loading plot representing phospholipids associated with each rice group endosperm. Blue and orange-colored data points represent each phospholipid related to, consecutively, general rice and sake rice. HK, *Hakutsurunishiki*; NB, *Nipponbare*; NS, *Nakate Shinsenbon*; YM, *Yamadanishiki*; YW, *Yamadawara;* PCA, principal component analysis.

calculation was performed to reduce high data dimension based on the average spectrum of each ROI.[43] All peaks associated with matrix clusters were excluded from the measurement.

As a result, clustering, as shown in score plots (Figs. 3A and 3C), demonstrated a clear separation along PC1 between sake rice and general rice in relation to phospholipid ions in the ROIs embryo and endosperm. Each peak associated with each rice cluster was indicated in the loading plots (Figs. 3B and 3D). To address the issue of peak selection derived from several aggregated and overlapping peaks, further filtering was performed by picking peaks with loading values higher than 0.05.

The distribution of phospholipids extracted from each area of interest is summarized in Table 1. Among all detected phospholipid types, the classes are grouped into fatty acylcarnitine, diacylglycerol (DAG), PC, PG, and PE. A total of 37 peaks were strongly correlated with embryos of *Hakutsurunishiki* and *Yamadanishiki* as sake rice group representatives, whereas 10 peaks were observed to be associated with the embryos *of Nipponbare, Nakate Shinsenbon*, and *Yamadawara* as the members of general rice group (Tables 1 and S2). It was obvious that the sake rice embryo showed dominant PCs, while that of general rice was rich in PEs. Furthermore, from the analysis of the endosperm region, a noticeable difference in the number of peaks was recovered between the 2 rice groups; 21 peaks were closely related to sake rice, while 49 peaks were found to be connected to general rice. Tables 1 and S3 indicated that PGs were found to be accumulated more than other phospholipids in the endosperm of sake rice. By contrast, the general rice endosperm contained a high abundance of DAGs and PCs. To provide a more detailed understanding of the actual accumulation of phospholipids, the abundance of each phospholipid type in rice cultivars was imaged.

Table 1. Distribution of phospholipids in sake rice and general rice based on regions of interest.

ROIs	Rice groups	Total PLs	Total each PLs species				
			Fatty acylcarnitines	DAGs	PCs	PGs	PEs
Embryo	Sake rice	37	2	0	22	10	3
	General rice	10	0	3	0	0	7
Endosperm	Sake rice	21	3	0	7	11	0
	General rice	49	4	19	16	2	6

DAGs, diacylglycerols; PCs, phosphatidylcholines; PEs, phosphatidylethanolamines; PGs, phosphatidylglycerols; PLs, phospholipids; ROIs, regions of interest.

Spatial distribution of phospholipids in embryo

A number of phospholipid peaks corresponding to each rice part of interest were visualized. Prior to image generation, we further highlighted the phospholipid representatives with only specific and clear localization. Out of 37 phospholipids found in the sake rice embryo, 2 fatty acylcarnitines, 22 PCs, 10 PGs, and 3 PEs (Tables 1 and S2), we selected 1 fatty acylcarnitine, 3 PCs, 2 PGs, and 1 PE to exemplify the distribution within the embryo (Fig. 4A). The phospholipids PC (32:4) *m/z* 764.463, PG (32:0) *m/z* 761.474, and PE (40:3) *m/z* 798.601 were solely distributed in the germ of *Hakutsurunishiki* and *Yamadanishiki* rice tissues, although PE (40:3) in *Yamadanishiki* rice, in particular, was found in lower abundance. Interestingly, PG (32:0) was observed not only dispersed in the germ but also predominantly discovered in the core of the *Hakutsurunishiki* rice. Albeit, according to the loading plot, being exclusive to the sake rice embryo, we also included the regional distribution information for the general rice germ to make a comparison. Phospholipids, including fatty acylcarnitine (23:5) *m/z* 502.330, PC (38:7) *m/z* 826.536, PC (38:8) *m/z* 824.520, and PG (38:4) *m/z* 798.601 were present not only in the germ of sake rice group but in the general rice as well, with slightly different intensities. For example, based on an overall visual, *Yamadawara* showed a lower accumulation compared to the other 4 types of rice. This supports the correspondence between these phospholipids with the sake rice embryos as presented in the score plot and loading plot of PCA.

Meanwhile, only 2 categories of phospholipid correspond to the general rice embryos among 10 detected phospholipids, namely DAGs and PEs (Tables 1 and S2). Furthermore, we chose 3 phospholipids from each class to be visualized, for instance, DAGs (34:2) *m/z* 615.496, DAG (34:1) *m/z* 617.512, DAG (36:4) *m/z* 617.514, PE (34:1) *m/z* 740.520, PE (34:0) *m/z* 742.538, and PE (36:2) *m/z* 744.554 (Fig. 4B). All examples were evidently accumulated in the germ of general rice tissues; however, *Yamadawara* exhibited another intriguing DAGs accumulation in the bran region, with high intensities. In comparison to the sake rice grains, *Yamadanishiki* showed a relatively high distribution of DAGs in the embryo and slightly lower in the bran area. Meanwhile, scarcity of the DAGs abundance was clear in the *Hakutsurunishiki* embryo and bran. While the presence of PEs in the regular rice embryo was apparent, it was barely visible in the sake rice germ. This result may suggest that DAGs and PEs are characteristics of the general rice embryos.

To wrap up this result, both rice groups exhibited various phospholipids in the germ region. According to a previous report,[44] PC, PE, PI, and PG, which were also detected in this study, except PI, were discovered to be the main lipids present in rice germ and bran, accounting for roughly 80%. As previously reported, these types of phospholipids PC, PG, and PE contributed to the decrease in important aroma compounds in sake.[10] Fortunately, the process of polishing may effectively eradicate them from the grains since they are dominantly accumulated in the outer layer areas. However, since fatty acylcarnitines and DAGs were also detected, mainly in the general rice samples, it might be necessary to further investigate the potential impacts of these phospholipids on the sake's quality.

Spatial distribution of phospholipids in endosperm

A total of 21 phospholipids associated with the sake rice endosperm mainly consist of PGs, followed by 7 PCs and 3 fatty acylcarnitines (Tables 1 and S3). Despite belonging to the same group, *Hakutsurunishiki* and *Yamadanishiki* displayed a distinguishable phospholipid distribution difference in the endosperm (Fig. 5A). As examples in *Hakutsurunishiki* rice, fatty acylcarnitine (25:1) *m/z* 506.361, PC (34:0) *m/z* 800.558, PC (32:0) *m/z* 734.569, PC (30:0) *m/z* 744.495, PG (36:3) *m/z* 773.533, and PG (38:3) *m/z* 801.564 primarily accumulate in the central region of the endosperm, in spite of a slight difference in the intensity. For example, PC (30:0) showed a lower intensity compared to the other previously mentioned phospholipids. In addition, a noticeable distribution of PC (34:0) and PG (38:3), respectively, was also observed in the embryo and extended beyond the core of the endosperm. Additionally, it is also important to note that PG (36:5) *m/z* 807.458 presented a recognizable occurrence toward the epical end of the *Hakutsurunishiki* grain tissue, which is the opposite side of the germ. Whereas the distribution of phospholipids in the endosperm of *Yamadanishiki* differs from that of *Hakutsurunishiki*, as they exhibited a scattered accumulation throughout the tissues rather than concentrated in the central part, with PC (32:0) and PC (30:0) generally showed higher intensities. Except for fatty carnitine (25:1), the abundance that was observed in the core of the *Yamadanishiki* endosperm was found to be relatively low.

When the spatial distribution of phospholipids corresponding with the sake rice endosperm was also tracked in the endosperm of *Nipponbare, Nakate Shinsenbon*, and *Yamadawara* as general rice examples, it suggested different spatial accumulation patterns and relatively low intensities (Fig. 5A). Fatty acylcarnitine (25:1) distribution with *m/z* 506.361 was almost negligible in all general rice sections. For the PC group, PC (34:0) *m/z* 800.558 was concentrated in the germ area instead of in the endosperm, with *Nakate*

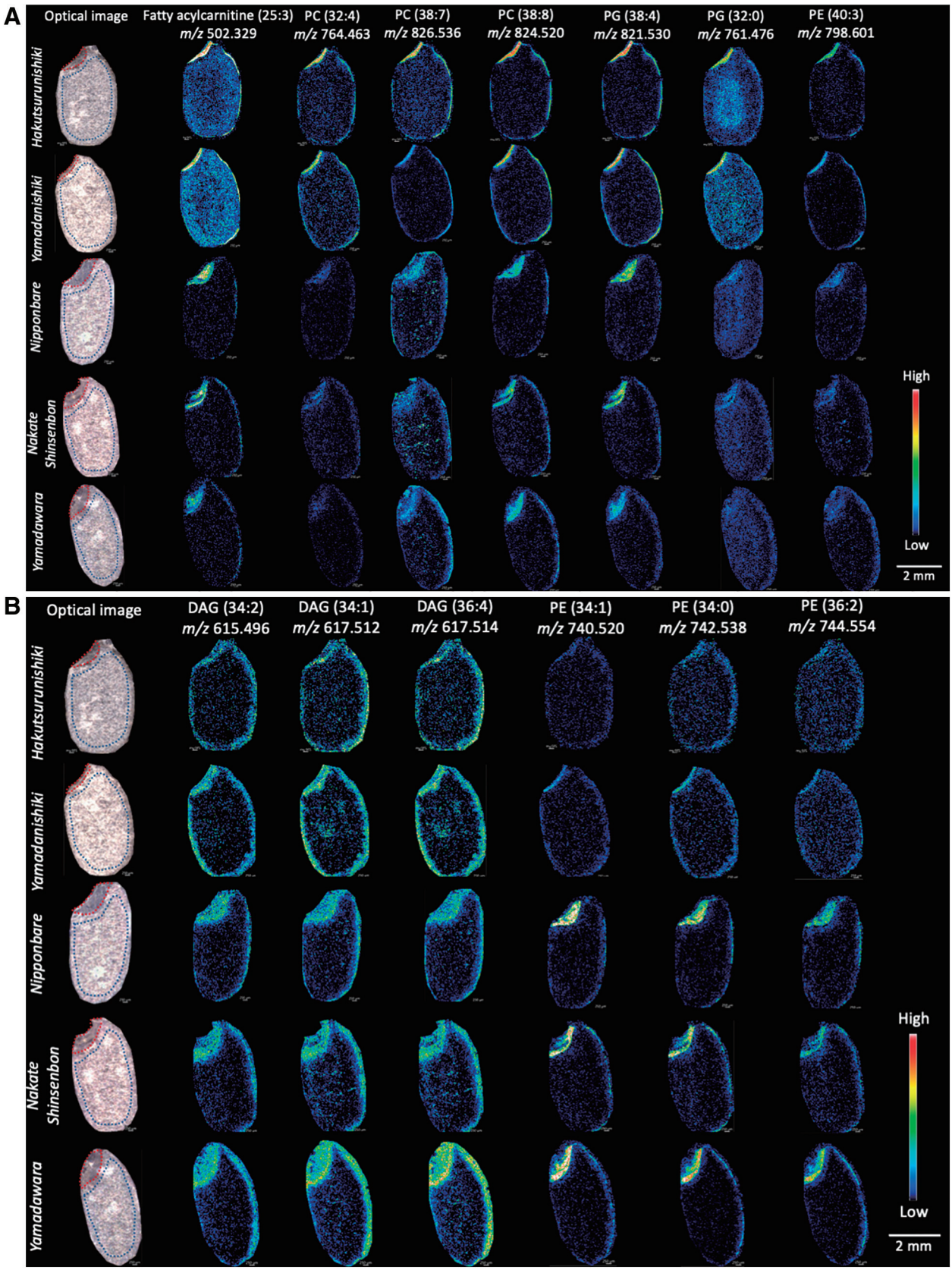

Fig. 4. Spatial distribution of representative phospholipids associated with sake rice embryo (A) and general rice embryo (B) obtained by MALDI MSI. MALDI, matrix-assisted laser desorption/ionization; MSI, mass spectrometry imaging.

Shinsenbon indicating the scarcity. PC (32:0) *m/z* 734.569 was only detected in the embryo and bran of *Yamadawara*, whereas PC (30:0) *m/z* 744.495 was minimally present in all general rice tissues. As in the case of PCs, PGs were also distributed distinctively. While *Nipponbare* and *Nakate Shinsenbon* exposed a clear presence of PG (36:5) throughout the endosperm, these 2 rice exhibit a very low abundance of PG (36:3) compared to *Yamadawara*. Lastly, PG (38:3) was

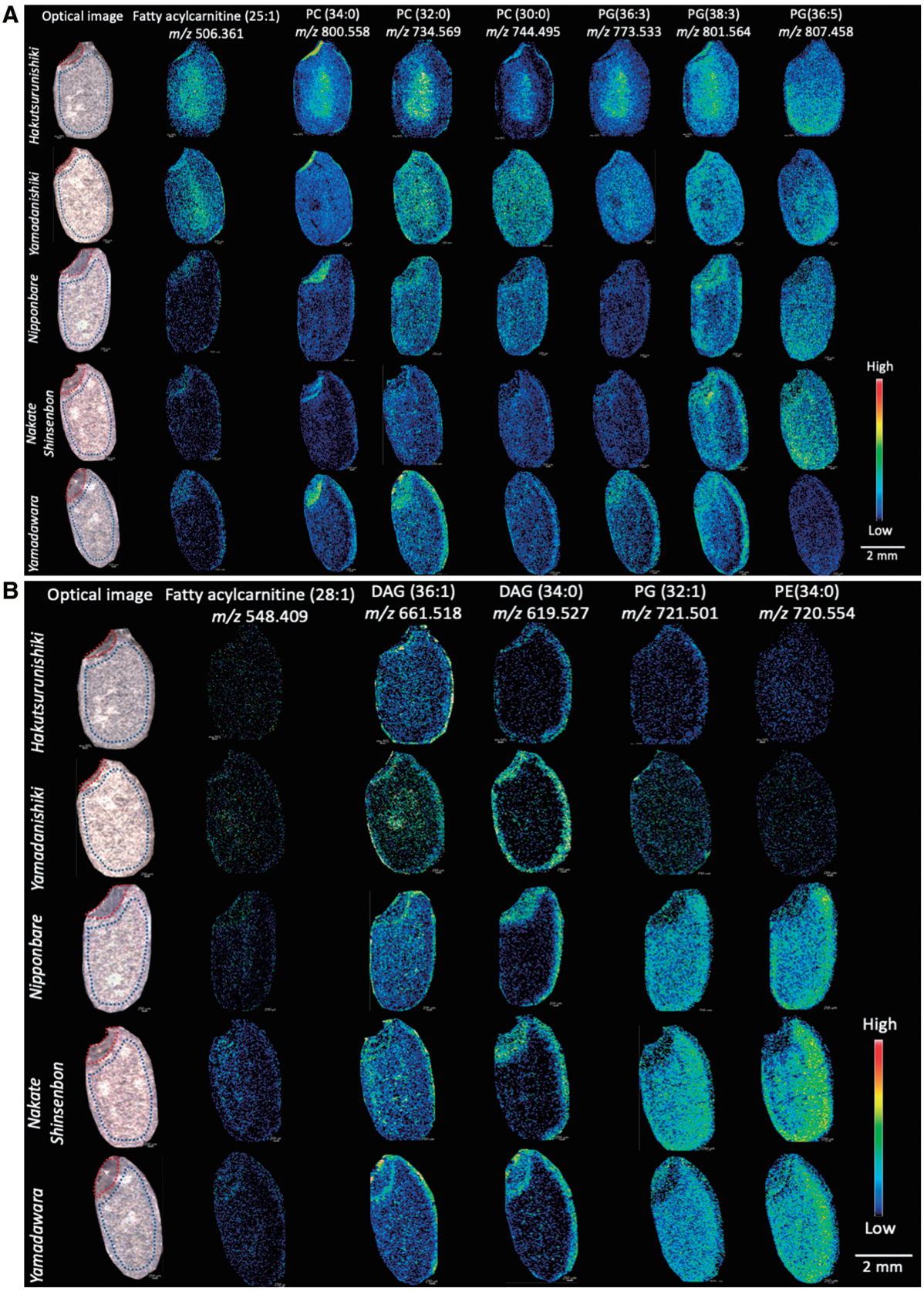

Fig. 5. Spatial distribution of representative phospholipids associated with sake rice endosperm (A) and general rice (B) obtained by MALDI MSI. MALDI, matrix-assisted laser desorption/ionization; MSI, mass spectrometry imaging.

distributed more in the bran area of *Nakate Shinsenbon* and *Yamadawara*.

Furthermore, we looked into the spatial distribution of phospholipids that potentially share a relationship with the endosperm of the general rice group and 49 phospholipids were extracted from the loading plot (Tables 1 and S3). This number was obviously greater in quantity compared to those of the sake rice endosperm. In terms of phospholipid variety,

the endosperm of general rice possessed more diverse phospholipids, including 4 fatty acylcarnitines, 19 DAGs, 16 PCs, 2 PGs, and 6 PEs. Five of the 49 phospholipid types such as fatty acylcarnitine (28:1) *m/z* 548.408, DAG (36:1) *m/z* 661.517, DAG (34:0) *m/z* 619.527, PG (32:1) *m/z* 721.501, and PE (34:0) *m/z* 720.554 were further visualized as presented in Fig. 5B. The distribution of PG (32:1) and PE (34:0) in all general rice samples is quite conspicuous and intriguing. These 2 phospholipids were evenly distributed throughout the entire endosperm, with higher abundance toward the bran of the dorsal areas of *Nakate Shinsenbon*. Similarly, *Yamadawara* also presented a heightened intensity of PE (34:0) in the bran region. On the other hand, it is essential to note that neither of the sake rice samples demonstrated the localization of PG (32:1) and PE (34:0), suggesting that these phospholipid types are probably specific to the endosperm of general rice. Moreover, 2 DAGs, DAG (36:1) and DAG (34:0), exposed different accumulation trends regardless of belonging to the same category. While the former did not exhibit localization, the latter was detected in the embryo and bran regions of all general rice. A similar distribution was also clear in the sake rice bran part, while that of *Hakutsurunishiki* was higher. Finally, none of the rice tissue sections accumulated fatty acylcarnitine (28:1).

From the results of this current study, it is shown that the distribution of phospholipids varied among rice groups and also between 2 sake rice cultivars. Even though we only captured the overall pattern in the phospholipid distribution across multiple rice cultivars commonly used in sake production as representatives and did not specifically address the individual structural and compositional variations, such as white core and nonwhite core region, among the rice cultivars, we recognize that such variation might be necessarily important as one of the potential factors may affect the differences in the distribution of phospholipids. Previous reports have linked the relationship between starch granules and lipids which then grouped lipids into starch lipids and non-starch lipids. The former lipids are those located in the starch granules, while the latter are found outside the starchy core, including those in the bran and germ.[7,45] As an example, fatty acids, lysophosphatidylcholine (LPC) and lysophosphatidylethanolamine (LPE) are well known as the principal starch lipids. In this study, *Hakutsurunishiki* rice was found to accumulate a higher abundance of PCs and PEs in the core of the endosperm, which may be suggested as starch lipids according to the theory. This finding may be explained by the previous report by Tamada *et al.*[46] that the *Hakutsurunishiki* grain possessed a larger starchy core (*shinpaku*) size that may influence the expression of starch lipids in the imaging data. On the other hand, *Yamadanishiki, Nipponbare, Nakate Shinsenbon,* and *Yamadawara* showed the primary accumulation of phospholipids outside of *shinpaku*, which were then possibly considered non-starch lipids. However, this is still a mere assumption according to the established theory and remains considered a limitation of our current work. Therefore, a more detailed analysis is necessary in the future to clarify how grain-by-grain variations contribute to the differences in the phospholipid distribution, such as comparative study of phospholipid distribution between white-core and non-white-core rice grains. In addition, there is still limited available literature providing quantitative values of phospholipid distribution in individual sake and general rice cultivars tested in this study. Up to the present, the previous reports only suggested a general quantity of lipids in brown rice, approximately 2%–3%, and such information in the tested rice still needs to be measured.

Visualization of spatial distribution of minerals

In this study, we focused on investigating the regional distribution of 12 minerals which included magnesium (Mg), phosphorus (P), potassium (K), iron (Fe), zinc (Zn), manganese (Mn), sulfur (S), calcium (Ca), sodium (Na), cobalt (Co), nickel (Ni), and silicon (Si) since the significance of these elemental components in sake's quality has been mentioned in previous studies.[13,21,47] For sake rice, we used all rice grain samples, while *Nipponbare* was the only general rice example. Using LA-ICP MSI technology, the information on the spatial distribution of the minerals was successfully detected (Fig. 6). The result suggested all investigated elements depicted identical distribution patterns among different rice groups, highly concentrated in the germs and slightly in the bran. The same trend was also observed in other minerals (Fig. S2). In addition, the distribution trend was observed similar to some lipid species, such as DAG. The similarity in spatial distribution is primarily due to their natural distribution patterns. In addition to that, the co-localization presumably may be attributed to their involvement in the lipid metabolism pathway. For example, the presence of P and Ca, respectively, is a crucial part of phospholipid structure and form interaction with the lipid membrane, directly affecting the spatial distribution.[48] Nevertheless, in terms of the concentration, it has been generally suggested that mineral concentration in brown rice usually used for sake material highly varies depending on the individual type of elements itself. For instance, the content of K and P was measured, ranging from 2000 to 3000 ppm and around 1000 ppm of Mg.[13] The rice cultivars examined also included *Yamadanishiki* and *Nipponbare*. Further study investigating the concentration of elemental components in other rice cultivars, including the ones used in this study, is highly recommended to explore, thus complementing the obtained information of the spatial distribution in this current result.

Finally, this study could provide information on the distribution of numerous phospholipids in the investigated rice grains. Sake rice and general rice showed different phospholipids distribution and similar mineral distribution. Referring to a previous work by Aramaki *et al.*[13] that showed the effect of polishing treatment on the concentration of elemental components, the elimination of those distributed throughout the germ and surface fractions of raw rice may be possibly polished at a minimum rate of 70%. Several minerals that predominantly exist in the germ and bran areas were drastically reduced and relatively leveled off after 70% polished. This polishing ratio may also be sufficient for removing phospholipids dispersed in the germ and bran. However, special attention is highly demanded for those located in the endosperm, especially in the central area, which will be potentially left after the polishing process. Since it is reasonably difficult to polish off, thereby, suitable strategies are worth the exploration as future perfectives. First, from the biological aspect, it might be necessary to investigate the environmental conditions where *Hakutsurunishiki* rice is cultivated, subsequently compared to the cultivation conditions of other rice cultivars containing a lower abundance of phospholipids in the core of endosperm

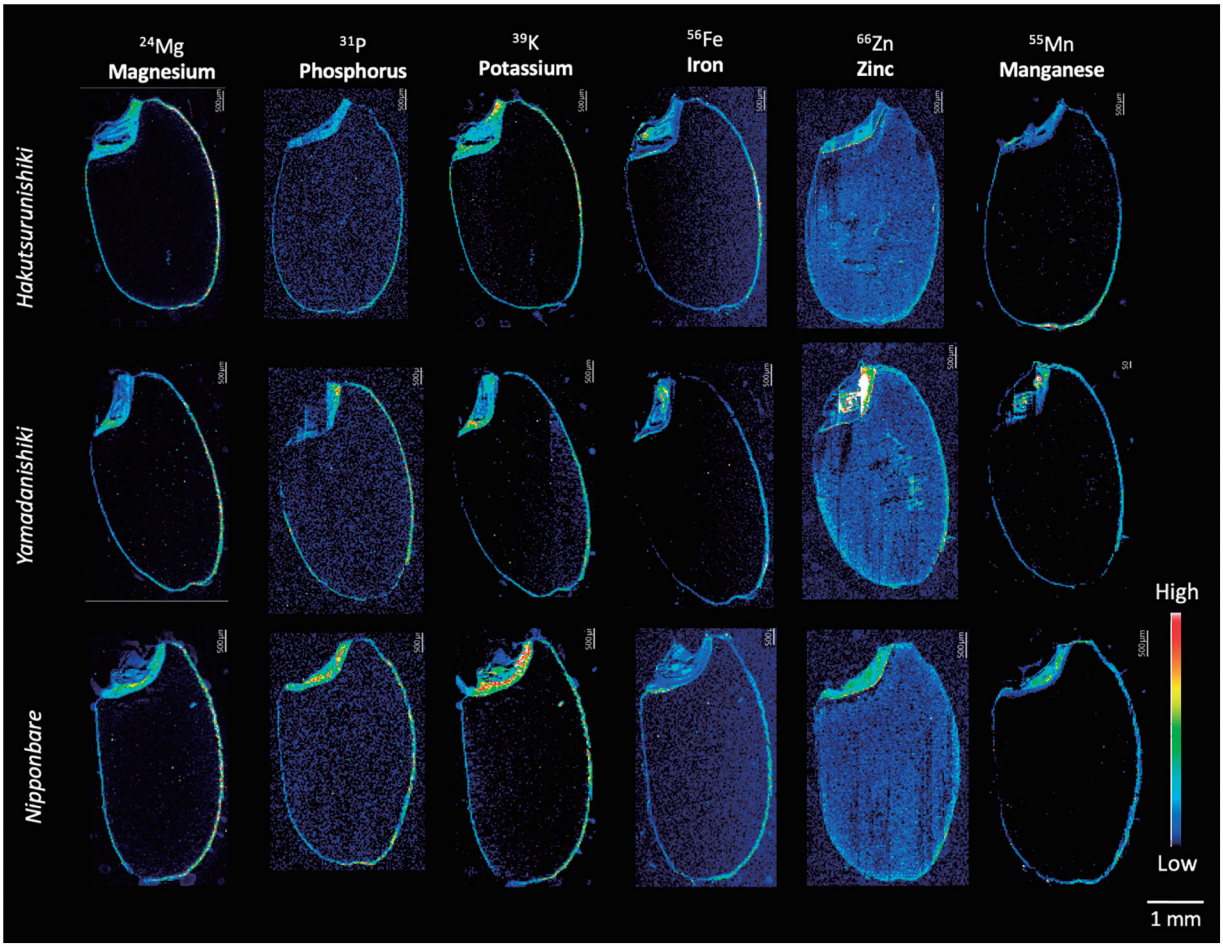

Fig. 6. Spatial distribution of representative minerals in sake rice (*Hakutsurunishiki* and *Yamadanishiki*) and a general rice example (*Nipponbare*) obtained by MALDI MSI. MALDI, matrix-assisted laser desorption/ionization; MSI, mass spectrometry imaging.

to find the optimal condition in achieving lower phospholipid abundance in the starch granule. Following this, development in the future breeding might also be promising. For example, among 5 rice cultivars used in this study, *Hakutsurunishiki* rice has the potential to be used as a parent and crossed with other cultivars with a lower abundance of endosperm phospholipids to produce rice with a lower content of phospholipids in the core endosperm.

CONCLUSION

In this study, we conducted a comprehensive investigation and visualization of a variety of phospholipids and minerals in brown rice utilized in sake manufacturing, as well as the spatial distribution. Detected phospholipids are including fatty acylcarnitine, DAG, PC, PG, and PE. Using specific regions, sake rice and general rice could be further discriminated based on their phospholipid accumulation. In terms of minerals, we observed 12 elements, namely Mg, P, K, Fe, Zn, Mn, S, Ca, Na, Co, Ni, and Si, with uniform distribution patterns across different rice cultivars. Both sake rice (*Hakutsurunishiki* and *Yamadanishiki*) and general rice (*Nipponbare, Nakate Shinsenbon*, and *Yamadawara*) exhibited distinct phospholipids profiles but similar distribution trends of elements. To the best of our knowledge, this is the first study that elucidates a more comprehensive view of the spatial distribution of phospholipids and minerals in brown rice as a raw material for sake production. This finding is expected to be valuable for sake breweries in the rice cultivars selection and polishing strategy; however, additional research is required in the future. However, while this study has successfully provided comprehensive phospholipid and mineral distribution in several rice cultivars for sake production, several limitations remain that need to be addressed. To gain a better understanding of the observed pattern of distribution, several potential factors, such as structural and compositional grain-by-grain variations, environmental and storage conditions, and quantitative values, warrant further exploration.

AUTHOR CONTRIBUTIONS

All authors designed the study; E. Farestiani, S.S., and K.O. conducted the experiments; Y.T., S.S., and E. Fukusaki supported the discussion; E. Farestiani and S.S. wrote the manuscript. All authors reviewed and approved the final manuscript.

DISCLOSURE STATEMENT

The authors declare no conflict of interest. This study will be incorporated into master's thesis, which will be submitted by E.F. to Osaka University as part of the requirements for her master's degree.

REFERENCES

1) M. Okuda. Rice used for Japanese sake making. *Biosci. Biotechnol. Biochem*. 83: 1428–1441, 2019.
2) S. Okada, M. Suehiro, K. Ebana, K. Hori, A. Onogi, H. Iwata, M. Yamasaki. Genetic dissection of grain traits in *Yamadanishiki*, an excellent sake-brewing rice cultivar. *Theor. Appl. Genet*. 130: 2567–2585, 2017.
3) A.-K. Horigane, K. Suzuki, M. Yoshida. Moisture distribution in rice grains used for sake brewing analyzed by magnetic resonance imaging. *J. Cereal Sci*. 60: 193–201, 2014.
4) K. Nagato, M. Ebata. Studies on White-Core Rice Kernel: II. On the physical properties of the kernel. *Jpn. J. Crop Sci*. 28: 46–50, 1959 (in Japanese).
5) M. Tamaki, S. Kurita, M. Toyomaru, T. Itani, T. Tsuchiya, I. Aramaki, M. Okuda. Difference in the physical properties of white-core and non-white-core kernels of the rice varieties for sake brewing is unrelated to starch properties. *Plant Prod. Sci*. 9: 78–82, 2006.
6) B.-O. Juliano. Lipids in rice and rice processing. In: *Lipids in Cereal Technology* (Ed: P. J. Barnes), Academic Press, London, 1983.
7) L. Liu, D.-L.-E. Waters, T.-J. Rose, J. Bao, G.-J. King. Phospholipids in rice: Significance in grain quality and health benefits: A review. *Food Chem*. 139: 1133–1145, 2013.
8) K. Sawada, H. Kitagaki. Residual mitochondrial transmembrane potential decreases unsaturated fatty acid level in sake yeast during alcoholic fermentation. *PeerJ* 4: e1552, 2016.
9) K. Takahashi, Y. Ohara, K. Sueno. Breeding of a sake yeast mutant with enhanced ethyl caproate productivity in sake brewing using rice milled at a high polishing ratio. *J. Biosci. Bioeng*. 123: 707–713, 2017.
10) K. Furukawa, T. Yamada, H. Mizoguchi, S. Hara. Increased alcohol acetyltransferase activity by inositol limitation in *Saccharomyces cerevisiae* in sake mash. *J. Biosci. Bioeng*. 96: 380–386, 2003.
11) K. Takahashi, F. Tsuchiya, A. Isogai. Relationship between medium-chain fatty acid contents and organoleptic properties of Japanese sake. *J. Agric. Food Chem*. 62: 8478–8485, 2014.
12) Y. Yamane, S. Takemiya, N. Kawase, H. Saiki. Sensory properties of some fatty acids in sake. *J. Brew. Soc. Jpn*. 92: 224–227, 1997 (in Japanese).
13) I. Aramaki, M. Ebe, T. Miura, M. Yoshii. Distribution of minerals in rice grains used for sake brewing. *J. Brew. Soc. Jpn*. 106: 837–847, 2011 (in Japanese).
14) A. Nose, T. Hamasaki, T. Takenaka, M. Hojo. Effect of water used in diluting alcohol content on the quality of Japanese sakes. *J. Brew. Soc. Jpn*. 108: 188–200, 2013 (in Japanese).
15) Y. Tamada, M. Tokui, N. Yamashita, T. Kubodera, T. Akashi. Analyzing the relationship between the inorganic element profile of sake dilution water and dimethyl trisulfide formation using multi-element profiling. *J. Biosci. Bioeng*. 127: 710–713, 2019.
16) S. Iino, M. Watanabe. Effects of *Moromi*-pressure at sake filtration on the quality of sake. *J. Brew. Soc. Jpn*. 84: 555–559, 1989 (in Japanese).
17) M. Tadenuma, S. Sato. Studies on the colorants in saké: Presence of ferrichrysin as iron containing colorant in Saké. *Agric. Biol. Chem*. 31: 1482–1489, 1967.
18) K. Takahashi, S. Sato, K. Nakamura, M. Tadenuma, T. Ozeki, K. Goto. Studies on changes in color and flavor of sake caused by exposure to light and storage (XV) effect of metals on changes in color by storage. *J. Soc. Brew. Jpn*. 66: 611–615, 1971 (in Japanese).
19) M. Okuda, M. Joyo, H. Fukuda. Changes in mineral concentrations during sake making. *J. Brew. Soc. Jpn*. 110: 431–443, 2015 (in Japanese).
20) M. Okuda, M. Joyo, H. Fukuda, N. Goto. Changes during polishing in mineral concentrations of rice grains used for sake making. *J. Brew. Soc. Jpn*. 109: 887–900, 2014 (in Japanese).
21) H. Soga, M. Furukawa, H. Kudo, K. Takahashi, K. Yoshizawa. Effect of minerals on rice digestion at sake brewing with puffed brown rice: Effect of mineral salts on sake making (Part 3). *J. Brew. Soc. Jpn*. 82: 646–650, 1987 (in Japanese).
22) L. Connolly, A. Jamzad, M. Kaufmann, C.-E. Farquharson, K. Ren, J.-F. Rudan, G. Fichtinger, P. Mousavi. Combined mass spectrometry and histopathology imaging for perioperative tissue assessment in cancer surgery. *J. Imaging* 7: 203, 2021.
23) A. Menetrey, R. Legouffe, A. Haouala, D. Bonnel, E. Rouits, J. Bosq, J. Stauber. Tumor distribution by quantitative mass spectrometry imaging of the inhibitor of apoptosis protein antagonist xevinapant in patients with resectable squamous cell carcinoma of the head and neck (EudraCT Number: 2014-004655-31). *Anal. Chem*. 94: 12333–12341, 2022.
24) M.-F. Rittel, S. Schmidt, C.-A. Weis, E. Birgin, B. van Marwick, M. Rädle, S.-J. Diehl, N.-N. Rahbari, A. Marx, C. Hopf. Spatial omics imaging of fresh-frozen tissue and routine FFPE histopathology of a single cancer needle core biopsy: A freezing device and multimodal workflow. *Cancers (Basel)* 15: 2676, 2023.
25) S. Ryu, M. Ohuchi, S. Yagishita, T. Shimoi, K. Yonemori, K. Tamura, Y. Fujiwara, A. Hamada. Visualization of the distribution of nanoparticle-formulated AZD2811 in mouse tumor model using matrix-assisted laser desorption ionization mass spectrometry imaging. *Sci. Rep*. 10: 15535, 2020.
26) S. Ikuta, E. Fukusaki, S. Shimma. Visualization of glutamate decarboxylase activity in barley seeds under salinity stress using mass microscope. *Metabolites* 12: 1262, 2022.
27) E. Takeo, E. Fukusaki, S. Shimma. Mass spectrometric enzyme histochemistry method developed for visualizing *in situ* cholinesterase activity in *Mus musculus* and *Drosophila melanogaster*. *Anal. Chem*. 92: 12379–12386, 2020.
28) A. P. Wisman, M. Minami, Y. Tamada, S. Hirohata, K. Gomi, E. Fukusaki, S. Shimma. Visualization of dipeptidyl peptidase B enzymatic reaction in rice *koji* using mass spectrometry imaging. *J. Biosci. Bioeng*. 134: 133–137, 2022.
29) A. Moreno-Pedraza, I. Rosas-Román, N.-S. Garcia-Rojas, H. Guillén-Alonso, C. Ovando-Vázquez, D. Díaz-Ramírez, J. Cuevas-Contreras, F. Vergara, N. Marsch-Martínez, J. Molina-Torres, R. Winkler. Elucidating the distribution of plant metabolites from native tissues with laser desorption low-temperature plasma mass spectrometry imaging. *Anal. Chem*. 91: 2734–2743, 2019.
30) A.-P. Wisman, E. Fukusaki, S. Shimma. Structure-based non-targeted mass spectrometry imaging analysis of dried long pepper (*Piper longum*). *ACS Food Sci. Technol*. 2: 872–877, 2022.
31) R. Pitchapa, S. Dissook, S.-P. Putri, E. Fukusaki, S. Shimma. MALDI mass spectrometry imaging reveals the existence of an *N*-acyl-homoserine lactone quorum sensing system in *Pseudomonas putida* biofilms. *Metabolites* 12: 1148, 2022.
32) A. Sakanaka, M. Kuboniwa, S. Shimma, S.-A. Alghamdi, S. Mayumi, R.-J. Lamont, E. Fukusaki, A. Amano. *Fusobacterium nucleatum* metabolically integrates commensals and pathogens in oral biofilms. *mSystems* 7: e00170–22, 2022.
33) J. Kokesch-Himmelreich, O. Wittek, A.-M. Race, S. Rakete, C. Schlicht, U. Busch, A. Römpp. MALDI mass spectrometry imaging: From constituents in fresh food to ingredients, contaminants and additives in processed food. *Food Chem*. 385: 132529, 2022.
34) S. Shimma. Mass spectrometry imaging. *Mass Spectrom. (Tokyo)* 11: A0102, 2022.
35) Y. Yoshimura, N. Zaima. Application of mass spectrometry imaging for visualizing food components. *Foods* 9: 575, 2020.
36) V. Pirro, L.-S. Eberlin, P. Oliveri, R.-G. Cooks. Interactive hyperspectral approach for exploring and interpreting DESI-MS images of cancerous and normal tissue sections. *Analyst* 137: 2374–2380, 2012.
37) P.-J. Trim, S.-J. Atkinson, A.-P. Princivalle, P.-S. Marshall, A. West, M.-R. Clench. Matrix-assisted laser desorption/ionisation mass spectrometry imaging of lipids in rat brain tissue with integrated unsupervised and supervised multivariant statistical analysis. *Rapid Commun. Mass Spectrom*. 22: 1503–1509, 2008.

38) S. Shimma, Y. Tamada, A. -P. Wisman, S. Hirohata, K. Gomi, E. Fukusaki. Visualization of phospholipids and glucose in rice *koji* using microscopic mass spectrometry imaging. *Shimadzu Application Note* (No. 64), 2021.
39) A.-P. Wisman, Y. Tamada, S. Hirohata, E. Fukusaki, S. Shimma. Metabolic visualization reveals the distinct distribution of sugars and amino acids in rice *koji*. *Mass Spectrom. (Tokyo)* 9: A0089, 2020.
40) N. Zaima, Y. Yoshimura, Y. Kawamura, T. Moriyama. Distribution of lysophosphatidylcholine in the endosperm of *Oryza sativa* rice. *Rapid Commun. Mass Spectrom*. 28: 1515–1520, 2014.
41) L.-A. McDonnell, R.-M.-A. Heeren. Imaging mass spectrometry. *Mass Spectrom. Rev.* 26: 606–643, 2007.
42) A. Guo, Z. Chen, F. Li, Q. Luo. Delineating regions of interest for mass spectrometry imaging by multimodally corroborated spatial segmentation. *Gigascience* 12: giad021, 2023.
43) E.-R. Muir, I.-J. Ndiour, N.-A. Le Goasduff, R.-A. Moffitt, Y. Liu, M.-C. Sullards, A.-H. Merrill, Y. Chen, M.-D. Wang. Multivariate analysis of imaging mass spectrometry data. BIBE 2007. Proceedings of the 7th IEEE International Conference on Bioinformatics and Bioengineering. 472–479, 2007.
44) H. Yoshida, T. Tanigawa, N. Yoshida, I. Kuriyama, Y. Tomiyama, Y. Mizushina. Lipid components, fatty acid distributions of triacylglycerols and phospholipids in rice brans. *Food Chem*. 129: 479–484, 2011.
45) W.-R. Morrison. Lipids in cereal starches: A review. *J. Cereal Sci*. 8: 1–15, 1988.
46) Y. Tamada, T. Asai, T. Kubodera, T. Akashi, E. Fukusaki, S. Shimma. Rice grain structural characteristics of sake rice cultivar *Hakutsurunishiki* for *daiginjo-shu* brewing. *Biosci. Biotechnol. Biochem*. 88: 445–452, 2024.
47) T. Fujitani. Biochemical studies on the mineral components in sake yeast: Part V. The relationship of the mineral composition of yeast to fermentation. *Agric. Biol. Chem*. 30: 925–930, 1966.
48) J.-M. Henschel, A.-N. Andrade, J.-B.-L. dos Santos, R.-R. da Silva, D.-A. da Mata, T. Souza, D.-S. Batista. Lipidomics in plants under abiotic stress conditions: An overview. *Agronomy (Basel)* 14: 1670, 2024.